Mon. Not. R. Astron. Soc. **000**, 000–000 (0000) Printed 5 February 2008 (MN LATEX style file v2.2)

An Infrared Imaging Survey of the Faint Chandra Sources near the Galactic Centre

R.M. Bandyopadhyay,[1⋆] J.C.A. Miller-Jones,[1,2] K.M. Blundell,[1] F.E. Bauer,[3] Ph. Podsiadlowski,[1] A.J. Gosling,[1] Q.D. Wang,[4] E. Pfahl,[5] and S. Rappaport[6]

[1] *Department of Astrophysics, University of Oxford, Keble Road, Oxford, OX1 3RH, UK*
[2] *Astronomical Institute "Anton Pannekoek", University of Amsterdam, Kruislaan 403, Amsterdam, The Netherlands, 1098 SJ*
[3] *Columbia Astrophysics Laboratory, Columbia University, 550 W. 120th St., New York, NY 10027, USA*
[4] *Dept. of Astronomy, University of Massachusetts, Amherst, MA 01003, USA*
[5] *Dept. of Astronomy, University of Virginia, Charlottesville, VA 22903, USA*
[6] *Center for Space Research, Massachusetts Institute of Technology, Cambridge, MA 02139, USA*

5 February 2008

ABSTRACT

We present near-IR imaging of a sample of the faint, hard X-ray sources discovered in the 2001 *Chandra* ACIS-I survey towards the Galactic Centre (GC) (Wang *et al.* 2002). These ∼800 discrete sources represent an important and previously undetected population within the Galaxy. From our VLT observations of 77 X-ray sources, we identify candidate K-band counterparts to 75% of the *Chandra* sources in our sample. The near-IR magnitudes and colours of the majority of candidate counterparts are consistent with highly reddened stars, indicating that most of the *Chandra* sources are likely to be accreting binaries at or near the GC.

Key words: binaries: close – infrared: stars – X-rays: stars – stars: mass loss

1 THE CHANDRA GALACTIC CENTRE SURVEY

The origin and contribution of diffuse and discrete X-ray sources to the X-ray spectrum and the total X-ray luminosity of the Galactic Plane have been a point of debate for decades. The unprecedented sensitivity and angular resolution of the *Chandra X-ray Observatory* has been utilized by Wang *et al.* (2002; hereafter W02) and Muno *et al.* (2003) to investigate the nature of this Galactic Centre (GC) X-ray emission. The W02 ACIS-I survey of the central $0.8^\circ \times 2^\circ$of the GC revealed a large population of previously undiscovered discrete weak sources with X-ray luminosities of $10^{32} - 10^{35}\,\mathrm{erg\,s^{-1}}$. The nature of these ∼800 newly detected sources, which may contribute ∼10% of the total X-ray emission of the GC, is as yet unknown. In contrast to the populations of faint AGN discovered from deep X-ray imaging out of the Galactic Plane, our calculations suggest that the extragalactic contribution to the hard point source population over the entire W02 survey is ≤ 10%, consistent with the $\log(N) - \log(S)$ function derived from the *Chandra* Deep Field data (CDF; Brandt *et al.* 2001). The harder (≥3 keV) X-ray sources (for which the softer X-rays have been absorbed by the interstellar medium) are likely to be at or beyond the distance of the GC, while the softer sources are likely to be foreground X-ray active stars or cataclysmic variables (CVs) within a few kpc of the Sun. The distribution of X-ray colours (Fig. 1) suggests that < 30% of the *Chandra* sources are foreground objects; a more detailed discussion of the X-ray source characteristics will be presented in Muno, Bauer, & Bandyopadhyay, (*in prep*).

Pfahl *et al.* (2002; hereafter PRP02) considered in detail the likely nature of these *Chandra* sources and concluded on the basis of binary population synthesis (BPS) models that many, if not the majority, of these systems are wind-accreting neutron star binary systems (hereafter WNS). Depending on the masses of the companions, the WNSs may belong to the "missing" population of wind-accreting Be/X-ray transients in quiescence, or to the progenitors of intermediate-mass X-ray binaries (IMXBs; $3 \leq M/M_\odot \leq 7$). The existence of tens of thousands of quiescent Be/XRBs in the Galaxy has been predicted since the early 1980s (Rappaport & van den Heuvel 1982; Meurs & van den Heuvel 1989), while it has only recently been recognized that IMXBs may constitute a very important class of XRBs that had not been considered before (King & Ritter 1999; Podsiadlowski & Rappaport 2000; Podsiadlowski *et al.* 2002). In a detailed population synthesis study of low- and intermediate-mass

⋆ email:rmb@astro.ox.ac.uk

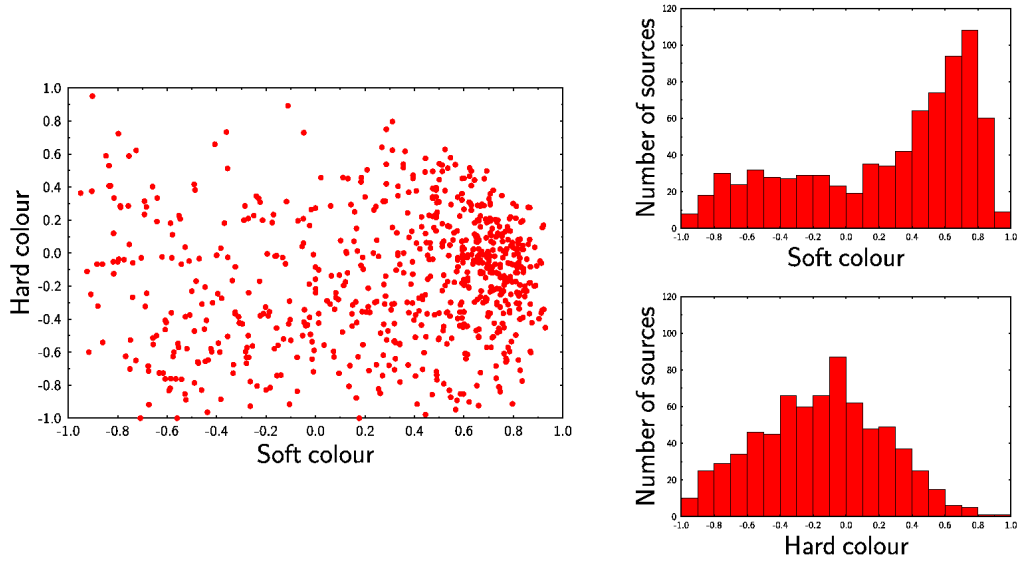

Figure 1. Characteristics of the X-ray source population detected in the *Chandra* mosaic. Left: colour-colour diagram. Right: histograms of the number of soft and hard X-ray sources in the GC field. The three X-ray bands are hard (H: 5-8 keV), medium (M: 3-5 keV), and soft (S: 1-3 keV). Soft colour is defined as *(M-S/M+S)*, and hard colour as *(H-M/H+M)*. The sources which are soft and thus most likely foreground objects are those located in the bottom left quadrant of the colour-colour diagram.

XRBs (L/IMXBs), Pfahl *et al.* (2003) found that 80-95 % of all L/IMXBs should in fact descend from intermediate-mass systems. The W02 *Chandra* survey may contain up to 10% of the entire Galactic population of WNSs. In addition to the WNSs, a fraction of the *Chandra* sources could be CVs (Ebisawa *et al.* 2005) or transient low-mass XRBs/black-hole binaries (PRP02; Belczynski & Taam 2004).

The first step in determining the nature of this population is to identify counterparts to the X-ray sources. These observations must necessarily be done in the infrared due to the high optical extinction in the direction of the GC. The successful achievement of our goals requires astrometric accuracy and high angular resolution to overcome the confusion limit of the crowded GC. The 2MASS survey has a limiting magnitude of K=14.3, and although the astrometric positions are accurate to 0.2″, the survey has a spatial resolution of $\geq$2″. As such, the 2MASS data are severely confusion limited in the GC and moreover are of insufficient depth to detect the majority of the expected counterparts. We therefore constructed a survey program using the ISAAC IR camera on one of the 8-metre telescopes of the Very Large Telescope (VLT) at the European Southern Observatory (ESO) in Chile, with the goal of obtaining high-resolution *JHK* -band images in order to identify a statistically significant number of counterparts to the X-ray sources on the basis of the *Chandra* astrometry.

2 IR OBSERVATIONS AND DATA ANALYSIS

In constructing our VLT/ISAAC program, we preferentially selected hard X-ray sources from the *Chandra* survey, as the soft sources are most likely to be foreground. For the early-type donors of the WNSs, we expect intrinsic magnitudes of K=11–16, with the peak of the magnitude distribution at K ∼14 (PRP02); these are therefore readily distinguishable from the majority of late-type donors expected in low-mass black hole or neutron star transient XRBs which generally have $K \geq$16 in quiescence. The average extinction towards the GC was expected to be A_K ∼2–3 (Blum *et al.* 1996, hereafter B96; Cotera *et al.* 2000; Dutra *et al.* 2003); therefore by imaging to a magnitude limit of K=20 we should detect most of the WNSs. At this limit we could also expect to identify some counterparts to the hard X-ray sources as AGN. However, there are no AGN with $K \leq$17 in the *Chandra* survey of the Hubble Deep Field North of Hornschemeier *et al.* (2001). Although we cannot rule out the possibility of detecting AGN with $K <$17, we expect these to be rare; therefore in most cases we expect AGN to be distinguishable from the WNSs, although further observations may be required to separate AGN from low-mass XRB counterparts. We further note that our IR observations indicate that there are patches in the observed fields where the extinction even in K is substantially larger than average (as high as $A_K \sim 6$; see *e.g.* B96), significantly reducing our detection sensitivity in the corresponding regions (see Section 3; a more detailed discussion of the GC extinction is presented in Gosling, Blundell, & Bandyopadhyay, *submitted*).

In 2003, we imaged 26 fields within the *Chandra* survey region with the VLT, containing a total of 77 X-ray point sources. We utilized ISAAC's 1024×1024 pixel Hawaii Rockwell detector, which provides a 2.5×2.5 arcmin field of view at a resolution of 0.1484″ per pixel. Images were obtained with $\lesssim$0.6″ seeing. For each field, four 90-second exposures were obtained per filter, with random offsets of ∼ 20″ between each exposure (using a standard ISAAC jitter template). Thus with a total of 6 minutes integration time per filter, the limiting magnitudes of our survey are J=23 (S/N=5), H=21, and K_s=20 (S/N=10).

The initial reduction of the images (including flat-fielding, removal of bad pixels, and sky subtraction) was performed using the ESO/ISAAC pipeline software. We then astrometrically locked the ISAAC images to the cor-

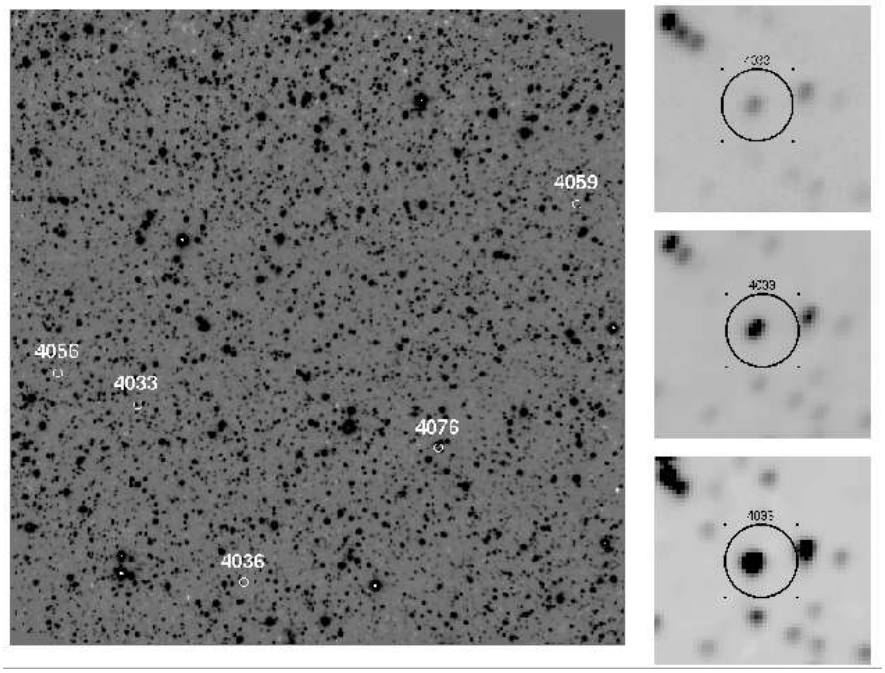

Figure 2. Left: an example ISAAC K_s-band field (2.5 arcmin^2), showing the positions of 5 *Chandra* X-ray sources. Right: Zoom-in view ($8''\times 8''$) of the $1.3''$ error circle of one of the *Chandra* sources in this field, overlaid on the J (top), H (middle), and K_s (bottom) ISAAC images.

responding 2MASS images, resulting in an astrometric accuracy of $0.2''$ for the VLT images. IR source positions and magnitudes were derived using the SExtractor package (version 2.3.2), which performs well in fields which are crowded but not confusion-limited, such as our ISAAC images (see the SExtractor manual for futher details: http://terapix.iap.fr/IMG/pdf/sextractor.pdf). Owing to the crowding in the field, a Mexican hat smoothing kernel of FWHM 2.5 pixels was used over a 7×7 pixel grid, with the "filtering" option activated. This option smooths the image before doing the candidate source detection, resulting in a gain in the ability to detect sources within crowded fields. After extensive trials to optimize detection of faint sources, the detection threshold was set to 1.15σ per pixel above the local background (sufficiently low to ensure we detected even the faintest sources), with a minimum area of 3 pixels (with all 3 greater than 1.15σ) required for a detection. The resultant source positions were then overlaid on the IR images, each of which was inspected by eye to ensure that the SExtractor positions corresponded to real sources in the field. In particular, the areas around the *Chandra* error circles were carefully inspected so that we were certain that none of the SExtractor-derived positions were spurious, but were indeed consistent with clearly visible IR sources.

Finally, we re-analyzed the W02 *Chandra* data to estimate the astrometric accuracy of the X-ray source positions. While the average "out-of-the-box" absolute astrometric accuracy for *Chandra* from the pipeline data processing is $0.6''$, we note that individual pointings can be off by up to several arcseconds (we have no way of knowing how good the *Chandra* accuracy is *a priori*). Unfortunately, because of the small number of X-ray sources per *Chandra* pointing with identified optical/IR counterparts (usually <2 X-ray/2MASS matches per pointing, which is insufficient to improve the *Chandra* pipeline astrometry) and the typical faintness of optical counterparts to Galactic X-ray sources such as expected here, we cannot establish the absolute astrometry for each tile of the survey; in fact it is even difficult to do so for the survey as a whole.

We refined the astrometric solution for the W02 mosaic by locking it to three significantly deeper single-pointing observations in the *Chandra* archive (each $17'\times 17'$) made within the survey region: these fields are Sgr A* (Muno *et al.* (2003), Sgr B2, and the Arches Cluster. The Sgr A* field astrometry was originally derived using three foreground stars, and later refined by matching 36 X-ray sources within $5'$ of the field centre to foreground stars in the 2MASS catalog (Muno *et al.* 2005). For the Sgr B2 and Arches fields, the astrometry was established using $\gtrsim 10$ X-ray/2MASS matches found within $5'$ of the field centre (Muno, Bauer, & Bandyopadhyay, 2005, *in prep*). Starting with the fields adjacent to the deep exposures and moving outward, we derived the astrometry of the W02 mosaic by matching X-ray source positions (obtained using the *Chandra wavdetect* routine) in each pointing to those of adjacent pointings. However, the positional accuracy of *Chandra* X-ray sources varies strongly as a function of both off-axis angle and source counts. Given that most of the matches between pointings made using this method were done with X-ray sources detected $\gtrsim 6'$ off-axis, the statistical uncertainty of the *wavdetect* positions of each source is significant. Thus the corrected astrometry is not substantially more accurate than the default pipeline values, with systematic errors of up to $1''$. We therefore conservatively use an astrometric accuracy of $1''$ for the X-ray source positions in the W02 mosaic. For those *Chandra* sources with IR stars within a $1.3''$ radius error circle (see Section 3), the average X-ray/IR offset is $0.77''$, consistent with our assumed *Chandra* astrometric accuracy.

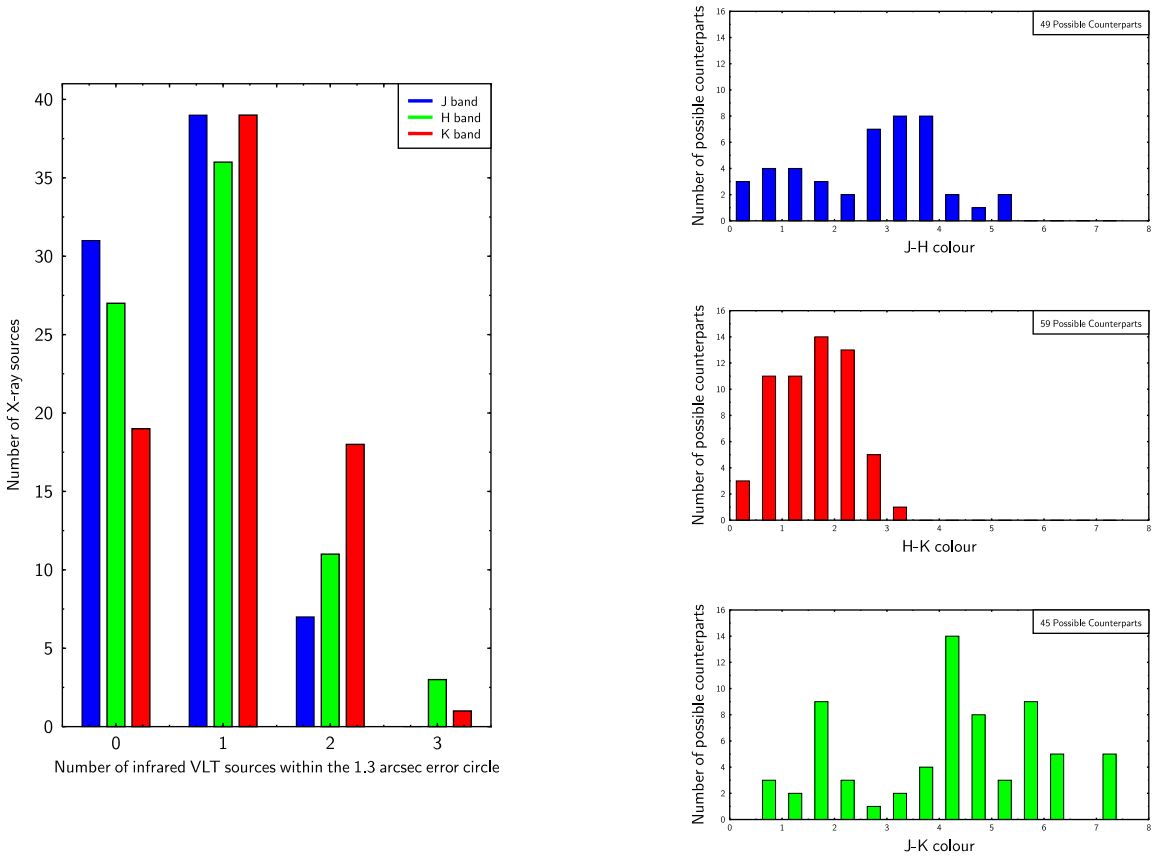

Figure 3. Left: histogram of the number of candidate IR counterparts per *Chandra* source within a 1.3″ radius error circle. Right: distribution of (reddened) IR colours of potential counterparts. The large spread of apparent colours is consistent with previously published photometry of GC stars (see *e.g.* B96).

3 RESULTS: IR CHARACTERISTICS

For 75% of the X-ray sources in our VLT fields, there are one or two resolved K_s-band sources within a 1.3″ error circle; only a small number of X-ray sources have more than two potential counterparts (Fig. 2); a complete list of all candidate IR counterparts is presented in Table 1. We use a radius of 1.3″ to account for the 1″ astrometric uncertainty of the *Chandra* data plus the uncertainty in the IR astrometry. As the ISAAC pixel size is $\sim 0.15''$, in order to entirely cover the IR astrometric uncertainty of 0.2″ it was necessary to expand the error radius by an integer number of pixels, resulting in an additional 0.3″ (2 pixels) being added to the 1″ X-ray error circle. Over 40% of the *Chandra* sources have no potential J-band counterparts, and only a few of the potential IR counterparts have colours consistent with unreddened foreground stars (Figs. 3 and 4). This is consistent with the expectation that the majority of the detected X-ray sources are heavily absorbed and thus are at or beyond the GC.

For an average GC extinction of A_K ∼3.3 (B96), the peak of the expected reddened K_s magnitude distribution for the WNSs is ∼17 (PRP02). The peak of the observed reddened K_s magnitudes for the potential counterparts (Fig. 6) is ∼16, with an *(H-K$_s$)* colour of ∼1.5–2.5 (Fig. 5). There is no obvious difference between the distribution of the *JHK* magnitudes of our candidate counterparts and those of the field population (Fig. 5); a more detailed comparison will be presented in a subsequent paper (Gosling *et al.* , *in prep*).

In order to determine the significance of the IR matches, a Monte Carlo simulation was carried out to see what fraction of randomly-located 1.3″-radius circles would contain an X-ray source simply by chance. The *Chandra* X-ray source positions were shifted by a random amount between 5″ and 20″, and the number of shifted error circles containing an IR counterpart was recorded. This procedure was carried out 10^4 times, and the results were binned according to the fraction of shifted positions whose error circles did not contain an IR source. The distribution obtained was then fitted with a normal distribution. The mean fraction of randomised positions with non-detections inside a 1.3″ error circle was found to be 0.253 ± 0.048, 0.405 ± 0.053, and 0.507 ± 0.053 for K_s, H, and J bands respectively (1σ errors). For comparison with the values obtained for the real data as reported below, these fractions correspond to approximately 25% (19 sources), 40% (31 sources), and 50% (39 sources) without counterparts in the simulated data, for K_s, H, and J respectively. Owing to the decreasing extinction with wavelength, the fraction of 1.3″ circles without IR counterparts decreased on moving from J through to K_s.

Out of a total of 77 X-ray source positions in our VLT fields, the percentage without IR counterparts in K_s, H, and J respectively were 25% (19 sources), 35% (27 sources), and 40% (31 sources; see Fig. 3), corresponding to 0.1-, 1.0- and

Table 1. Coordinates of Candidate IR Counterparts

Chandra X-ray source	K_s-band RA (J2000)	candidate[a] Dec (J2000)	*Chandra* X-ray source	K_s-band RA (J2000)	candidate[a] Dec (J2000)
CXOUJ174521.9-290519	17 45 21.9	-29 05 19	CXOUJ174536.5-284122	17 45 36.6	-28 41 21
CXOUJ174518.2-290405	17 45 18.2	-29 04 04	CXOUJ174454.2-285841	17 44 54.2	-28 58 42
	17 45 18.2	-29 04 06	CXOUJ174534.1-291327	17 45 34.1	-29 13 27
CXOUJ174517.2-290439	17 45 17.2	-29 04 40	CXOUJ174457.3-290614	17 44 57.4	-29 06 14
	17 45 17.2	-29 04 39		17 44 57.3	-29 06 13
CXOUJ174517.3-290625	17 45 17.3	-29 06 25	CXOUJ174455.2-290417	17 44 55.2	-29 04 17
CXOUJ174503.8-290051	17 45 03.8	-29 00 50		17 44 55.2	-29 04 16
CXOUJ174608.2-290622	17 46 08.2	-29 06 23	CXOUJ174449.9-291327	17 44 49.9	-29 13 27
CXOUJ174559.5-290601	17 45 59.5	-29 06 02	CXOUJ174428.7-285651	17 44 28.7	-28 56 52
CXOUJ174521.9-290617	17 45 21.9	-29 06 16		17 44 28.8	-28 56 51
CXOUJ174516.8-290541	17 45 16.8	-29 05 42	CXOUJ174459.8-291941	17 44 59.8	-29 19 41
CXOUJ174458.1-290509	17 44 58.0	-29 05 10	CXOUJ174457.6-292028	17 44 57.7	-29 20 28
	17 44 58.1	-29 05 09	CXOUJ174515.8-291723	17 45 15.8	-29 17 22
CXOUJ174459.9-290418	17 44 59.9	-29 04 18	CXOUJ174501.4-291933	17 45 01.4	-29 19 34
	17 44 59.9	-29 04 19	CXOUJ174450.9-291849	17 44 50.9	-29 18 49
CXOUJ174459.3-290050	17 44 59.2	-29 00 51	CXOUJ174429.1-291946	17 44 29.0	-29 19 46
	17 44 59.3	-29 00 50	CXOUJ174414.3-292610	17 44 14.4	-29 26 11
CXOUJ174638.3-285609	17 46 38.3	-28 56 09	CXOUJ174453.7-291952	17 44 53.7	-29 19 51
CXOUJ174638.7-285452	17 46 38.7	-28 54 50		17 44 53.6	-29 19 53
	17 46 38.8	-28 54 52	CXOUJ174429.6-291908	17 44 29.6	-29 19 08
CXOUJ174835.1-282336	17 48 35.0	-28 23 35		17 44 29.7	-29 19 07
CXOUJ174708.3-281410	17 47 08.2	-28 14 11	CXOUJ174434.1-291816	17 44 34.2	-29 18 16
	17 47 08.3	-28 14 10	CXOUJ174432.1-291801	17 44 32.1	-29 18 01
	17 47 08.3	-28 14 09	CXOUJ174507.4-291557	17 45 07.4	-29 15 57
CXOUJ174645.2-281547	17 46 45.3	-28 15 46	CXOUJ174354.7-290908	17 43 54.7	-29 09 09
	17 46 45.3	-28 15 48		17 43 54.8	-29 09 08
CXOUJ174658.0-281414	17 46 58.0	-28 14 14	CXOUJ174355.3-290954	17 43 55.3	-29 09 54
	17 46 57.9	-28 14 14	CXOUJ174425.9-293849	17 44 25.9	-29 38 48
CXOUJ174557.6-281955	17 45 57.6	-28 19 56	CXOUJ174403.6-292742	17 44 03.5	-29 27 43
CXOUJ174552.4-282027	17 45 52.4	-28 20 28		17 44 03.6	-29 27 43
	17 47 12.8	-28 48 06		17 44 03.6	-29 27 41
	17 47 12.7	-28 48 07	CXOUJ174407.0-292803	17 44 07.1	-29 28 04
CXOUJ174710.1-284931	17 47 10.1	-28 49 31	CXOUJ174412.3-292636	17 44 12.2	-29 26 36
	17 47 10.0	-28 49 30	CXOUJ174428.5-293929	17 44 28.4	-29 39 29
CXOUJ174706.3-284907	17 47 06.2	-28 49 07	CXOUJ174216.0-293756	17 42 16.0	-29 37 56
CXOUJ174703.1-284913	17 47 03.2	-28 49 13		17 42 15.9	-29 37 58
	17 47 03.2	-28 49 12	CXOUJ174216.1-293732	17 42 16.0	-29 37 33
CXOUJ174712.3-284828	17 47 12.3	-28 48 28		17 42 16.2	-29 37 32
CXOUJ174702.5-285258	17 47 02.4	-28 52 58	CXOUJ174210.4-293639	17 42 10.3	-29 36 40
CXOUJ174536.9-284013	17 45 36.9	-28 40 12			

[a]Note that for some *Chandra* sources there is more than one potential K_s-band counterpart. For these X-ray sources there are multiple entries in the Table, each entry showing the coordinates for a unique K_s-band candidate counterpart to that *Chandra* source.

2.0-σ below the expected values for a random distribution of X-ray error circles. These values are consistent with what is expected as a result of the stellar density in our fields. The average separation of stars in the K_s-band is 1.94″, thus with a 1.3″ error circle we would not expect a statistically significantly larger number of counterparts than for a random distribution. However, in the H- and J-band, where the average stellar separation is 2.29″ and 2.72″ respectively, we do expect to see a larger number of X-ray/IR matches than would be expected by chance, and indeed, that is what is observed. At the shorter wavelengths, we are detecting more sources within the X-ray error circles than would be expected by chance, and therefore we are likely to be detecting some of the true IR counterparts to the X-ray sources.

The detection of a larger number of potential counterparts in J and H (8 and 4 more sources, respectively, than in the simulated data) than would be expected from a random distribution has two potential interpretations. First, we may be detecting more matches of X-ray sources to foreground (rather than GC) stars, as foreground stars are subject to much less extinction. The second possibility is that there are a larger number of potential counterparts which are intrinsically brighter and bluer than the average field population, a result which would be consistent with the hypothesis that many of these faint *Chandra* sources may be WNS systems. In any case, this simulation shows that some fraction of the potential counterparts within the error circles are likely to be chance coincidences, especially at K, so follow-up spectroscopy must be used to identify which IR sources are the true counterparts to the X-ray sources.

There are no K_s-band counterparts for ∼25% of the *Chandra* sources. This is larger than the expected fraction

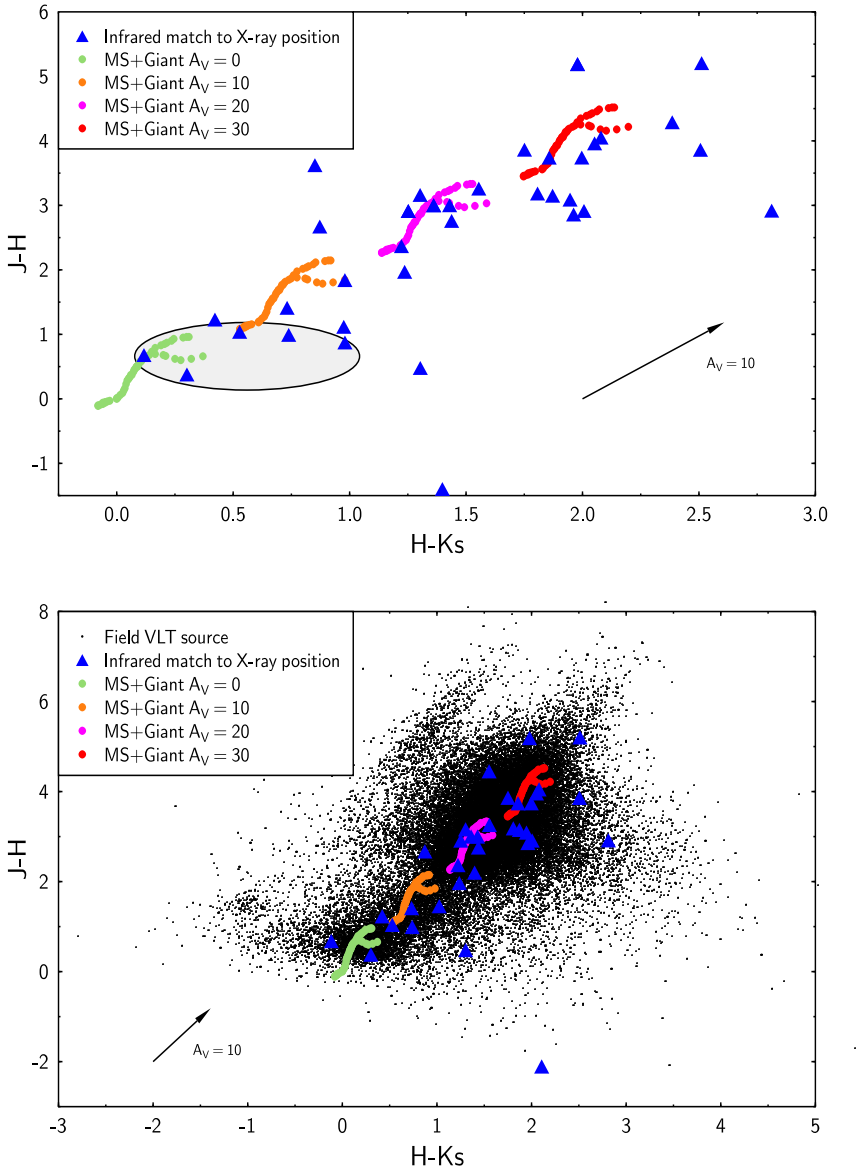

Figure 4. *Top:* Colour-colour diagram of all potential IR counterparts to the *Chandra* sources for which we have full three-colour information. The shaded oval indicates where unreddened AGN/QSOs would most likely be located (see text). The theoretical main sequence and giant branches are indicated at visual extinctions of 0, 10, 20, 30 ($A_K/A_V = 0.11$). *Bottom:* Colour-colour diagram showing all sources in our VLT fields. This illustrates that the vast majority of field stars are consistent with highly reddened stars; thus most of the stars (including potential X-ray counterparts) are at the distance of the GC (or beyond).

of background AGN from the CDF estimate, though other groups have predicted larger fractions (up to 50%). However, the extinction in the GC is extremely variable, even at K. From visual inspection of our VLT data it is clear that some areas exhibit larger than average extinction ($A_K \geq 5$) in the form of dust patches and lanes (Gosling, Blundell, & Bandyopadhyay, *submitted*). Seven of our X-ray sources are in regions of unusually heavy IR (notably K-band) extinction; thus we estimate that the true fraction of *Chandra* sources without counterparts at the limiting K_s magnitude of our survey is ∼16%. As has been noted by previous authors (B96; Cotera *et al.* 2000), the highly variable and structured nature of the extinction in the GC makes derivation of reddening-corrected photometry for the field population non-trivial. Thus a detailed assessment of the likely spectral types for the candidate counterparts will be presented by Gosling *et al.* (*in prep*).

4 DISCUSSION

The colours and magnitudes of the IR candidate counterpart population are generally consistent with main-sequence and giant stars at distances of the GC. Only a few sources have low extinctions consistent with foreground stars. Of the detected candidate counterparts, only a few have colours and magnitudes consistent with AGN/quasars; however these are indistinguishable from foreground stars on the basis of

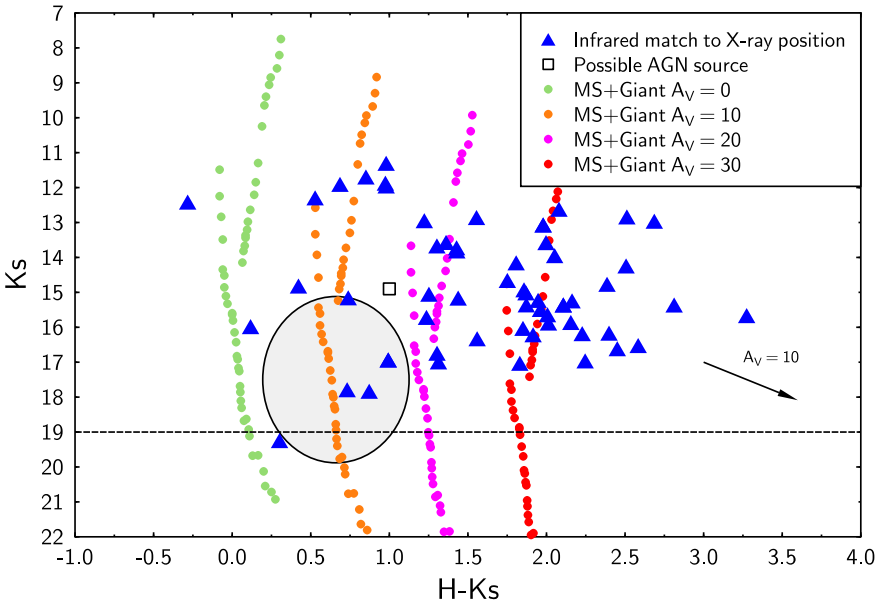

Figure 5. $H-K_s$ vs. K_s colour-magnitude diagram for all candidate IR counterparts to the *Chandra* sources (uncorrected for reddening). Theoretical main sequence and giant branches and AGN/QSO locus indicated as in Fig. 3. The small square indicates IR candidate counterpart for an X-ray source in the *Chandra* mosaic whose position is consistent that of a radio source for which an AGN identification is claimed (Bower *et al.* 2001). The dashed line shows a conservative estimate for the K_s 10σ detection limit of our VLT images.

magnitudes and colours alone. From visual inspection of our VLT images, none of the candidate counterparts appears intrinsically extended (though this of course does not rule out QSO or faint AGN). In Figs. 4 and 5 we have indicated the likely colours and magnitude range for AGN/QSOs (as derived from Spinoglio *et al.* 1995, Ivazic *et al.* 2001, Sharp *et al.* 2002, and Pentericci *et al.* 2003). Note that for substantial visual extinction ($A_V \geq$10) most extragalactic counterparts to the *Chandra* sources will be below the detection limits (Fig. 5) of our survey. The limiting magnitude of this survey also places limits on the types of stars detectable at the distance of the GC. Along the line of sight out to the distance of the GC, in our images we expect to detect all evolved (supergiant and giant) stars, but we will only detect main sequence stars of type G or earlier; K, M dwarfs in the GC will be below our detection limit.

On the basis of this astrometry and photometry, we were awarded VLT time in the summer of 2005 to obtain ISAAC K-band spectra of the 31 best candidate counterparts (K_s magnitudes ∼12–17); the goal of these observations is to identify the X-ray source counterparts via detection of accretion signatures. The primary accretion signature in the K-band which distinguishes a true X-ray counterpart from a field star is strong Brackett γ emission; this technique of identifying XRB counterparts has been verified with observations of several well-studied GC XRBs (see *e.g.* Bandyopadhyay *et al.* 1999). As these *Chandra* sources are weaker in X-rays than the previously known population of Galactic XRBs, and thus have lower inferred accretion rates, their emission signatures will likely be somewhat weaker than in the more luminous XRB population. However, the Brackett γ accretion signature is clearly detected in the IR spectra of CVs, which are only weak X-ray emitters with a similar X-ray luminosity range to the *Chandra* sources (see Dhillon *et al.* 1997 for IR emission signatures in CVs). Of course, the magnitude limits of our VLT imaging preclude detecting IR counterparts to any CVs which may be present in our fields located beyond a few kpc from the Sun. The comparison between CVs and the counterparts of the *Chandra* sources at GC distances is made purely to illustrate that even for X-ray binaries accreting at lower rates than in "canonical" systems, we expect the Brackett γ signature to be detected and thus the spectroscopic identification to be definitive even for these low-luminosity X-ray sources. The spectra we obtain of our brighter targets will allow us not only to identify the counterpart via its emission signature but also to spectrally classify the mass donors if absorption features are detected, a crucial step in determining the nature of this new accreting binary population.

Identifying IR counterparts to these newly discovered X-ray sources provides a unique opportunity to make a census of the various populations of accreting binaries in the GC and may ultimately allow a determination of each system's physical properties. As this *Chandra* survey may contain up to 10% of the entire population of accreting binary systems in the Milky Way (PRP02), our results will have important implications for our understanding of XRBs in the Galaxy, including their formation, evolutionary history, and physical characteristics. In particular, if many of the detected sources do indeed turn out to be the missing progenitors of L/IMXBs, it would put strong constraints on models of this important population of X-ray sources.

5 ACKNOWLEDGMENTS

The authors would like to thank Niel Brandt for helpful discussions about *Chandra* data analysis and astrometric is-

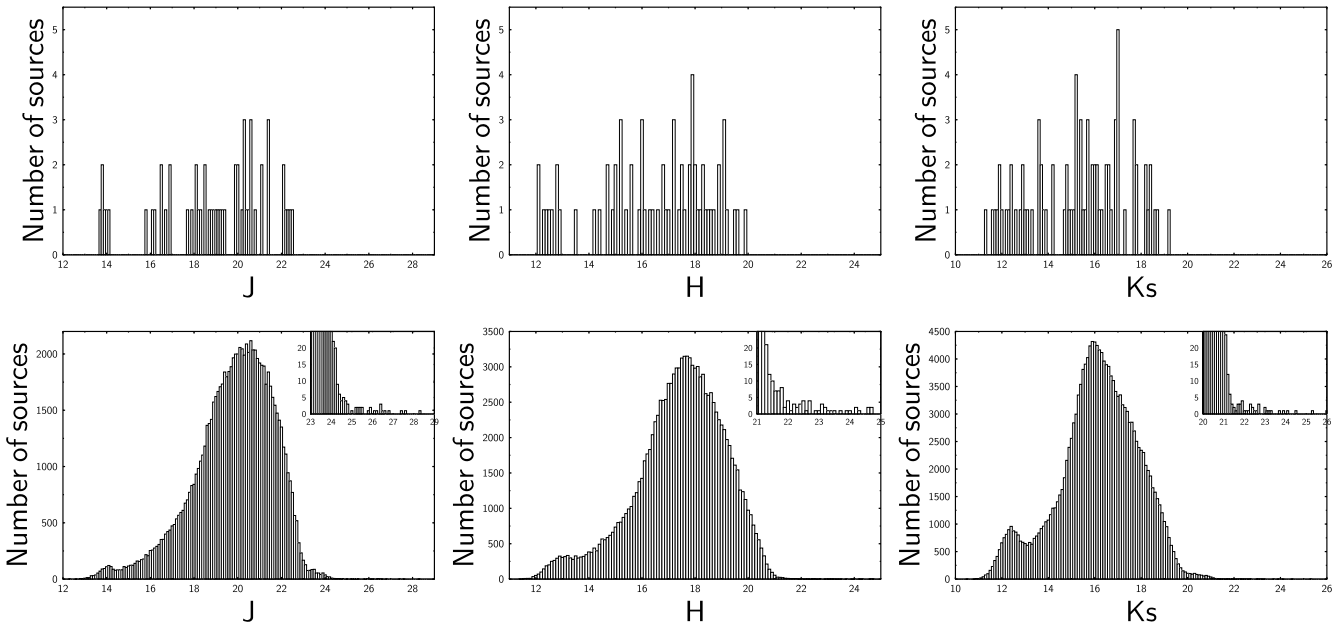

Figure 6. Histograms of JHK_s (reddened) magnitudes of the candidate counterparts to the *Chandra* sources (upper panels) and the field source population (lower panels).

sues, and Michael Muno for information about the astrometry of the *Chandra* image of Sgr A*. K. M. B. thanks the Royal Society for a University Research Fellowship. J. C. A. M.-J. and A. J. G. thank the UK Particle Physics and Astronomy Research Council for Studentships. We also thank Mark Morris for his helpful and rapid referee report. This paper is based on observations made with the ESO VLT at Paranal under program ID 71.D-0377(A).

REFERENCES

Bandyopadhyay, R.M., Shahbaz, T., Charles, P.A., & Naylor, T., 1999, MNRAS, 306, 417
Belczynski, K. & Taam, R.E., 2004, ApJ, 616, 1159
Blum, R.D., Sellgren, K., & DePoy, D.L., 1996, ApJ, 470, 864 (B96)
Bower, G.C., Backer D.C., & Sramek, R.A., 2001, ApJ, 558, 127
Brandt, W.N., *et al.* , 2001, AJ, 122, 2810
Cotera, A.S., Simpson, J.P., Erickson, E.F. & Colgan, S.W.J., 2000, ApJSS, 129, 123
Dhillon, V.S., *et al.* , 1997, MNRAS, 285, 95
Dutra, C.M., Santiago, B.X., Bica, E.L.D., & Barbuy B., 2003, MNRAS, 338, 253
Ebisawa, K., *et al.* , 2005, ApJ, *in press* (astro-ph/0507185)
Gosling, A.J., Blundell, K.M., & Bandyopadhyay, R.M., *submitted.*
Hornschemeier, A.E., *et al.* , 2001, ApJ, 554, 742
Ivazic, Z., *et al.* , 2001, Proc. IAU Symposium 184, p. 137
King, A.R. & Ritter, H., 1999, MNRAS, 309, 253
Meurs, E.J.A. & van den Heuvel, E.P.J., 1989, A&A, 226, 88
Muno, M.P., *et al.* , 2003, ApJ, 589, 225
Muno, M.P., Lu, J.R., Baganoff, F.K., Brandt, W.N., Garmire, G.P., Ghez, A.M., Hornstein, S.D., Morris, M.R., 2005, ApJ, *in press* (astro-ph/0503572)
Pentericci, L., *et al.* , 2003, A&A, 410, 75
Pfahl, E., Rappaport, S., & Podsiadlowski, Ph., 2002, ApJL, 571, L37 (PRP02)
Pfahl, E., Rappaport, S., & Podsiadlowski, Ph., 2003, ApJ, 597, 1036
Podsiadlowski, Ph. & Rappaport, S., 2000, ApJ, 529, 946
Podsiadlowski, Ph., Rappaport, S., & Pfahl, E., 2002, ApJ, 565, 1107
Rappaport, S. & van den Heuvel, E.P.J., 1982, Proc. IAU Symposium 98, p. 327
Sharp, R.G., Sabbey, C.N., Vivas, A.K., Oemler Jr., A., McMahon, R.G., Hodgkin, S.T., & Coppi, P.S., 2002, MNRAS, 337, 1162
Spinoglio, L., Malkan, M.A., Rush, B., Carrasco, L., & Recillas-Cruz, E., 1995, ApJ, 453, 616
Wang, Q.D., Gotthelf, E.V., & Lang, C.C., 2002, Nature, 415, 148 (W02)